# Microstructural, Mechanical and Wear behavior of in-situ Al-$TiB_2$ composites

**M.K. Hullur[1*], Dayanand M. Goudar[2], Julfikar Haider[3], S.A. Kori[3]**

[1]*Research Scholar, Baveshwar Engineering College Bagalkot, Karnataka, India,*

[2]*Tontadarya College of Engineering, Gadag, Karnataka, India*

[3]*Department of Engineering, Manchester Metropolitan University, Chester Street, Manchester, M1 5GD, UK*

[4]*Central University of Andhra Pradesh, AP, India*

**Abstract:** In this study, mechanical and wear properties of in-situ stir cast Al-$TiB_2$ composites were investigated. The composites were prepared by a metal salt reaction with different (3.0, 5.0 and 7.0 wt %) $TiB_2$ contents. The microstructure of the composites were examined through an optical and scanning electron microscopy (SEM/EDS). The microstructures clearly revealed the uniform distribution of $TiB_2$ particles in the Al matrix. The hardness of the in-situ Al-$TiB_2$ based composites increased by 42%, 55%, and 58% compared to the matrix with the addition of 3, 5, and 7 wt% $TiB_2$ reinforcements, respectively. The tensile strength of the 3, 5, and 7 wt% $TiB_2$ stir-cast composites increased by 25%, 33%, and 45%, respectively, compared to the matrix, whereas the ductility decreased by 4.9%, 24.3%, and 41.3%, respectively. A pin-on-disk tester was used to perform a dry sliding wear test at different loads and sliding speeds. In comparison to the Al matrix, the composite materials showed improved wear resistance. Furthermore, in the entire applied loads and sliding velocities, the wear rate decreased with the increase in $TiB_2$ content. The composites displayed lower wear rates due to their high hardness and strong interfacial bonding between the in-situ reinforcement and the matrix alloy.

**Keywords:** In-situ composite, Microstructure, Hardness, Tensile strength, Ductility, Wear rate

## 1. Introduction

Aluminum metal matrix composites (AMCs) are utilized extensively in the fields of aerospace, automotive, chemical, and transportation because of their outstanding mechanical strength, low density, high thermal conductivity, and thermal characteristics [1]. Al-matrix composites reinforced with ceramic particles have been developed to enhance mechanical and wear properties. The majority of the studies over the past few decades have been focused on the inclusion of reinforcing particles like SiC, $B_4C$, $Al_2O_3$, TiC, and graphite in the aluminium matrix or its alloys [2].Titanium Diboride ($TiB_2$) is a material with a very high melting point, great strength, and high wear resistance both at ambient and high temperatures.$TiB_2$is applied in armour components, cutting tools and crucibles due to its high density, high elastic modulus, and high compressive strength.$TiB_2$ is employed in forming composite materials, where its presence increases the matrix's strength and fracture toughness when combined with mainly other oxide ceramics[3].The Hamaker constant of $TiB_2$ is very close to that of molten aluminum and the other ceramic reinforcements. Thus, $TiB_2$is an attractive strengthening agent for aluminum-based composites [4,5]. The $TiB_2$ substance does not exist in nature, but it can be made through the carbo-thermal reduction of $TiO_2$ and $B_2O_3$. Different processes such as casting, powder metallurgy, infiltration, and spray deposition, can be used to synthesize the AMCs. These methods produce composites with poor properties due to poor cohesion at the reinforcement-matrix interface caused by improper wetting of the former by the latter and undesirable products of interfacial reactions, mechanical incompatibility and a large difference in the thermal expansion coefficients of the reinforcing particles and the matrix [6].

In-situ composites have gained a lot of attention recently, mostly because of their excellent mechanical characteristics, smooth interfaces between the reinforcement and the matrix, strong bonding with the matrix, and affordable manufacturing [7].Lakshmi et al. [8] used an in-situ reaction procedure using $K_2TiF_6$ and $KBF_4$ salts to produce AMC with $TiB_2$ reinforcement. Kori et al. [9] produced in-situ Al-5% $TiB_2$metal matrix composite (MMC) by melting Al-3.45%Ti and A1-1.55%B master alloy for 60 min at 1000°C.The fine $TiB_2$ particles and $Al_3Ti$ phase are formed in-situ via $K_2TiF_6$ and $KBF_4$ salt reaction in the Al alloys. However, the presence of the $Al_3Ti$ phase in Al-$TiB_2$ composites, degrade the overall mechanical properties of the composite. The $Al_3Ti$ formation in Al-$TiB_2$ composites can be prevented by increasing the reaction time, increasing the temperature, and limiting the salt fraction [10]. Feng et al. [11] employed in-situ

salt metal reactions to produce an Al-$TiB_2$ composite by adding potassium fluoride salts containing Ti and B to the hot aluminum melt. The interactions between the salts result in the creation of fine and homogeneous $TiB_2$ particles in the matrix. Kumar et al. [12] successfully produced the hypoeutectic Al-Si alloy reinforced with in-situ $TiB_2$ particles using the salt reaction technique. It was concluded that the in-situ composites possess mechanical properties that are noticeably superior to those of the base alloy. In another study [13], the reaction $TiO_2$, $H_3BO_3$, and $Na_3AlF_6$in Al melt was used to manufacture the in-situ Al-$TiB_2$ composite. It was observed that the composite tensile and yield strength increased significantly as the $TiB_2$ content increased. Manoj et al. [14] investigated the effect of $TiB_2$ particles on the morphology and mechanical behavior of Al-7075 composite with different wt. % of 2, 4, 6 and 8 wt.% $TiB_2$ produced using the stir casting process. It was reported that a reduction in grain size was observed owing to an increase in the wt. % of the $TiB_2$ particles. The addition of $TiB_2$ particles also increased tensile strength and microhardness as they form a strong interface and share the load with the matrix. The exothermic reaction time is a key factor in determining the size and shape of the precipitation particles [15, 16]. According to Madhavan et al. [17], higher particle nucleation was observed in the composites processed at 750$^oC$ for 60 min, and an increase in the percentage of $TiB_2$ particles produced finer and more spherical particles. Liu et al. [18] reported that with a reaction time of 60 min, the formation of large $TiB_2$ particles with a size of 1-2 µm and agglomeration in the matrix occurred. Mallikarjun et al. [19] studied in-situ A-2014/$TiB_2$ composites manufactured by the exothermic reaction of halide salts ($K_2TiF_6$ and $KBF_4$) at 850°C.It has been reported that when the duration of exothermic reaction increased, the volume of $TiB_2$ increased while the grain size decreased. Wu et al. [20] studied microstructure and mechanical properties of A356/$TiB_2$ composites synthesized by the salt metal reaction. It was observed that UTS and Young's modulus of the composites increased with an increasing wt.% of the $TiB_2$ particles. However, Poisson's ratio and yield strength decreased with the increasing wt.% of $TiB_2$ particles. In addition, the mechanical properties of the composite materials can be improved by grain refinement through heat treatment. Kumar et al. [12] investigated the wear behavior of an Al-7Si/$TiB_2$ composite produced by salt reaction. It was observed that the hardness, strength, and the wear resistance of the composites improved as their $TiB_2$ content increased.

Due to its ease of manufacture and low cost, the stir casting process remains the most researched technology for manufacturing AMCs. The stir casting method was used to create AMC, which combined the metallurgical qualities of the matrix and reinforcements and found use in cylinder liners, gear components, brakes, roller skates, pistons, bicycle frames, and baseball shafts. For the most uniform mixing of reinforcement particles in the matrix, the stir casting process has been found to be effective [21,22]. Moreover, the stir casting has been found to improve the wettability of molten metal with ceramic particles [23].The $TiB_2$reinforced $AMC_S$ produced using the stir casting process results in favorable interfacial reactions and created strong bonds between the Al matrix and reinforcement particles.

A number of studies published results concerning manufacturing, mechanical, and wear characteristics of the in-situ Al alloy/$TiB_2$composites. However, very limited information is available on the synthesis of in-situ composites made from pure Al/$TiB_2$.Tee et al. [24] reported that the in-situ-composite of high $TiB_2$ content (15wt.%) results in the formation of dendrite plates of $Al_3Ti$ particles, hinders the distribution of $TiB_2$ particles and exhibit low ductility owing to the fracturing of $A_3Ti$ flakes. The formation of large blow holes and brittle castings results from exceeding the wt% of $TiB_2$ in-situ by more than 10% [25]. It is, therefore, desired to maintain the $TiB_2$ content below 10 wt.%. The present work aimed to produce in-situ $TiB_2$ particles while adding $K_2TiF_6$ and $KBF_4$ salts to Pure Al matrix.

In the present study, the Al$x$$TiB_2$ in-situ composites were fabricated using a stir-casting process with varying weight percentages ($x$=3, 5, and7wt. %) of $TiB_2$. The novelty of the work is to use economically available halide salts and to study the mechanical and wear behaviour. The influence of $TiB_2$ incorporation on the microstructure, mechanical and wear properties was investigated. The study has a lot of potential for industrial applications because the Al-$TiB_2$ composites can be fabricated in-situ in a cost-effective manner.

## 2. Experimental details

### *2.1. Manufacturing of composite samples*

A commercially available pure Al alloy (CPA1) (99.7%) was selected as the matrix material and its chemical composition is shown in Table 1. The chemical composition of commercially available pure alloy, inorganic salt $KBF_4$($KBF_4$≥ 99.80%, $Fe_2O_3$≤ 0.05, $H_2O$ ≤ 0.15) and

$K_2TiF_6$($K_2TiF_6$ ≥99.80%, $Fe_2O_3$≤ 0.05, $H_2O$≤ 0.15) powders, assessed using Atomic Absorption Spectroscopy. The calculated amount of chemicals incorporated into the molten Al to form $TiB_2$ (3, 5 and 7wt.%) are given in Table 2. The pure Al (99.7) ingot was melted in an electrical heated crucible furnace (Make: FURMACO) to 750 °C. To enhance the wettability between the metal matrix and dispersion phase, the ready-mixed $KBF_4$ and $K_2TiF_6$ powders are preheated to a temperature of 200ºCadded into the melt and a chemical reaction with the melt synthesized $TiB_2$ particles. The reaction time was kept at 60 min [17] and the melt was stirred intermittently for 60min using a mechanical stirrer to form the $TiB_2$ particles with hexagonal and spherical morphology, and to distribute homogeneously within the matrix [26]. The melt temperature was measured using a K-type thermocouple (chromel–alumel).Before pouring, the melt was degassed using hexa-chloroethane ($C_2Cl$) tablets to avoid casting defects.

The formation of in-situ endogenous $TiB_2$ particles using the inorganic salts melt through chemical reaction can be written as [26].

$$3K_2TiF_6+13Al=3Al_3Ti+3KAlF_4+K_3AlF_6$$

$$2KBF_4+3Al=AlB_2+2KAlF_4$$

$$AlB_2+Al_3Ti=TiB_2+4Al \quad (1)$$

*Table 1. The chemical composition of pure Al (CPAl) cast*

| Element | Si | Fe | Mg | Fe Cu | Zn | Ti | Mn | Al |
|---|---|---|---|---|---|---|---|---|
| Wt.% | 0.15 | 0. 16 | 0.01 | .01 | 0.04 | 0.01 | 0.03 | Bal |

*Table 2. The quantity of inorganic salts used*

| $TiB_2$ (wt.%.) | 3 | 5 | 7 |
|---|---|---|---|
| $K_2TiF_6$ (grams) | 104 | 173 | 243 |
| $KBF_4$ (grams) | 131 | 220 | 304 |

The melt was poured into a cylindrical graphite mold to produce low porosity sound castings (Figure1b) with a diameter of 50 mm and a length of 300 mm. Overall stability (expansion

coefficient of graphite lower than that of steel) and very low porosity of the graphite allow the mold to retain their shape filled with molten metal.


*Figure1. (a) Electrical melting furnace with mechanical stirrer (b) cylindrical castings*

The samples were prepared using standard metallographic techniques of polishing on emery paper with 1/0, 2/0, 3/0 and 4/0 specifications for microstructural characterization. The micro polishing was carried out on a double-disc micro polishing machine (Metatech DM-2T). Mirror polishing was done using Levi-Gated liquid alumina on a velvet cloth, and diamond paste (0.5-2µm) on a PSA-coated velvet cloth with Aero-spray. The methanol washed polished samples are etched with Keller's reagent (1% vol. hydrofluoric acid, 15% vol. hydrochloric acid, 2.5% vol. nitric acid and water).

### *2.2. Sample characterization*

Metallographic observations were performed using an optical light microscope (ZYNAX and Clemex image analysis system) and a field emission Scanning Electron Microscope (SEM/EDS) (JEOL JSM-6480LV). The micro hardness is evaluated using a Vickers hardness tester (Meta-tech). The tests were performed on polished specimens with a weight of 150g for 10 seconds. Six measurements was taken from different locations on the specimen, and the average values along with the standard deviations were reported as the final hardness value of the composites.Standard tensile specimens were prepared from both the composites and base material by a CNC turning machine (Figure 2) and experiments were performed according to the ASTM E8M standard at ambient temperature using a universal tensile machine (UNITEK-9450PC, Blue Star India Ltd.) with a strain rate of $10^{-3}s^{-1}$. Three samples were used for each test condition to ensure data reproducibility.


*Figure 2. Standard tensile testing specimen*

### *2.3. Wear testing*

Dry sliding wear tests on the base alloy and composites were carried out in accordance with ASTM G-99 standards using a Pin-on-Disc type (TRE-20 DUCOM) wear testing equipment as shown in Figure 3 under dry sliding conditions. The disc was made of EN32 and had a hardness of 62 HRC. Base alloy and composite pin samples with diameters of 8 mm and a length of 30 mm were prepared. The wear test is performed at different loads (10, 20, 30 and 40 N) and sliding velocities (1,2 and 3.0 m/s). Weight loss during the wear test after a sliding distance of 2000 m at each load and sliding velocity were measured before and after the test using a high precision digital weighing machine (WENSAR, PGB-301, 0.01 mg accuracy).

*Figure 3. Pin-on-Disc wear testing machine*

## 3. Results and Discussion

### *3.1. Microstructural characteristics*

Figure 4(a) shows optical microstructure of the cast pure Al alloy with α-dendrite structure. The $TiB_2$ particles in the Al-3% $TiB_2$ composite are well distributed in the matrix with sizes ranging from 1 to 10μm. The dendrite size of the Al matrix is depicted finer compared to the base, which is due to the kinetics associated with the formation of $TiB_2$inthe matrix during the solidification. It is observed that in the Al-5%$TiB_2$and Al-7%$TiB_2$composites (Figure 4c and Figure4d),the amount and size of $TiB_2$ particles increase with the increasing $TiB_2$wt%.Clustering of the $TiB_2$ particles is also observed in some areas in the Al-7wt.% $TiB_2$ composite.

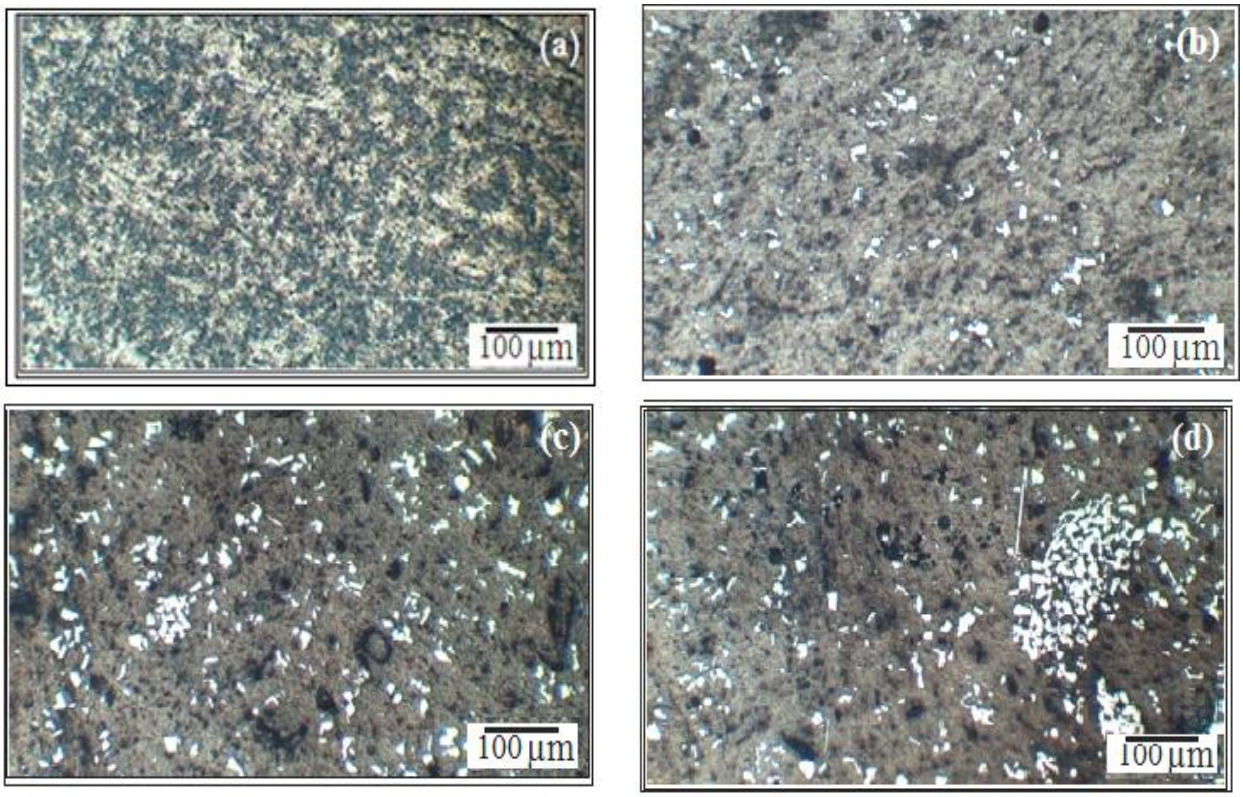


*Figure 4.Optical microstructures of (a)Pure Al, (b) Al-3wt.%$TiB_2$ (c) Al-5wt.%$TiB_2$ and (d) Al-7wt.%$TiB_2$composites*

SEM micrographs of pure Al and Al-$TiB_2$ in-situ composites is shown in Figure5 (a-d). Figure 5(a) shows the microstructure of pure Al. The α-phase shows the dendrite form of Al grains. It is observed that the $TiB_2$ particles in Al-3wt.%$TiB_2$(Figure 5b) and Al-5%wt. $TiB_2$ (Figure 5c)are formed into fine particles and most of which are segregated at α-Al grain boundaries. The $TiB_2$ particles formed are very fine in size in the range of 0.5-10μmand distributed at the grain boundaries and the nano-sized $TiB_2$ particles remain within Al grains of the α-Al matrix.SEM

micrograph of Al-7wt.%$TiB_2$ composite (Figure 5d) clearly exhibits high content and large agglomerations of $TiB_2$ particles with an increase in size. Because of their size and density, these massive agglomerations may not have been sufficiently separated by mechanical stirring [18]. SEM/EDS micrograph of Al-7wt.%$TiB_2$ composite shows formation of $TiB_2$ particles, presence of some $Al_3Ti$ residual phase and $AlB_2$ remain in the composite.

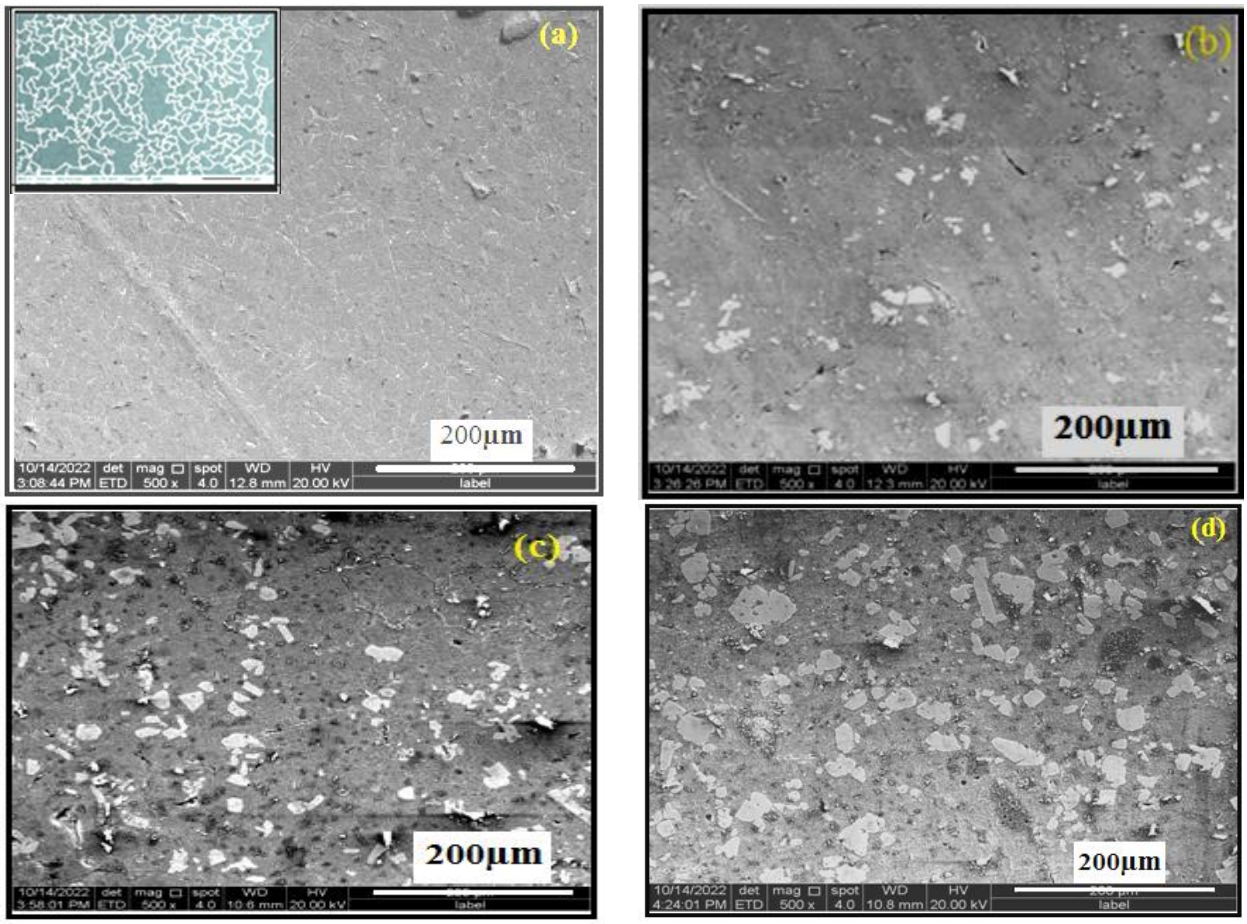


*Figure5. (a) SEM microstructures with an inverse map figure of Pure Al, (b) Al-3wt.%$TiB_2$composite, (c) Al-5wt.%.$TiB_2$composite, and (d) Al-7w.t%$TiB_2$composite*

Several parameters influence the size and distribution of $TiB_2$ particles, such as, cooling rate, in-situ reaction conditions and solute content [28]. The process begins with an in-situ reaction between the atoms of Ti and B, and as a result of atomic diffusion in the melt, $TiB_2$ micro particles are formed. There are still too many titanium and boron atoms in the bath, despite the production of nano$TiB_2$ particles. The remaining atoms will be absorbed by $TiB_2$ synthesis to grow particles during the succeeding diffusion process. Due to the reduced wettability between the $TiB_2$ particles and molten Al, the coarse $TiB_2$ particles are pushed towards the solid/liquid

interface and eventually distributed at the grain boundaries and overlapping regions, while the $TiB_2$ nano particles remain within the grains. Because $TiB_2$ is formed within the melt, the risk of particle oxidation is also minimized, improving wettability, and therefore, distribution. Increased volume fraction reinforcement in the matrix and clustering of $TiB_2$ particles are also observed in some areas with higher $TiB_2$ wt.%. Furthermore, the SEM/EDX spectrum of Al-3wt.%$TiB_2$in-situ composite (Figure 6) clearly shows the presence of Ti and B elements along with Al. The elemental mapping based on the EDS spectrum for Al-7wt.%$TiB_2$ composite is shown in Table 3.

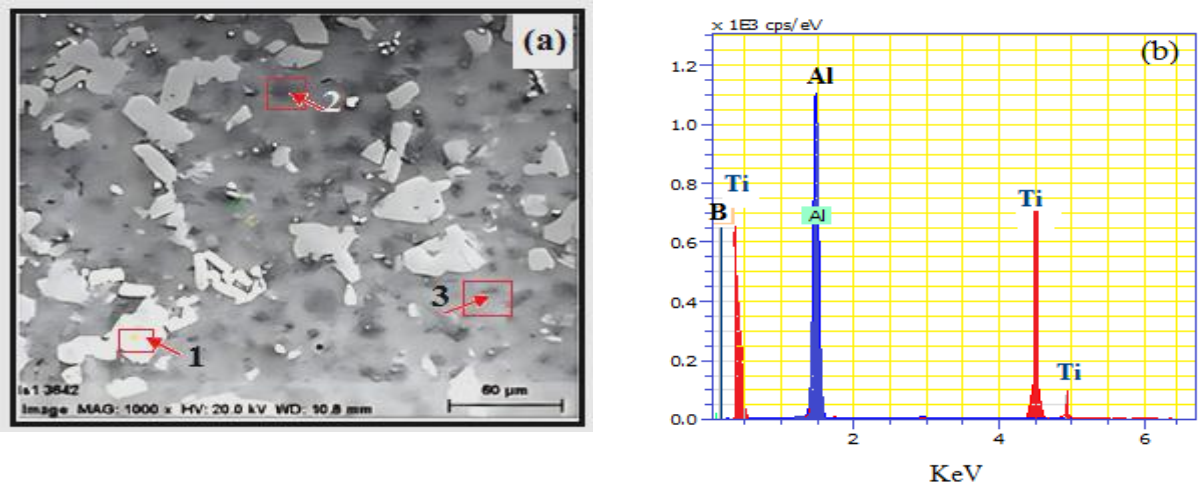


*Figure6. SEM/EDS micrograph of Al-7wt.%$TiB_2$ and (b) EDS spectrum.*

*Table3. Phase composition of EDS analysis of Al-7wt.% $TiB_2$composite*

| EDS spot | Phase | B | Ti | Al |
|---|---|---|---|---|
| 1 | $TiB_2$ | 31.39 | 67.58 | - |
| 2 | $Al_3Ti$ | - | 27.99 | 72.01 |
| 3 | $Al_2B$ | 16.95 | 0.14 | 82.91 |

### *3.2. Hardness and mechanical strength*

Figure7shows Vickers hardness values of both Al and Al-$TiB_2$in-situcomposites. Hardness improvements of 42%, 55% and 58.7% were obtained with 3wt%, 5wt%, and 7wt. % $TiB_2$ in-situ composites respectively. Due to the addition of hard particles to a soft matrix, composite materials produce a high degree of hardness. The hard $TiB_2$ improves the matrix material's hardness by improving its resistance to deformation [27]. Another aspect contributing to the

increase in hardness brought on by the homogenous distribution of in-situ $TiB_2$ particles in the Al matrix and particulate strengthening effect [14].

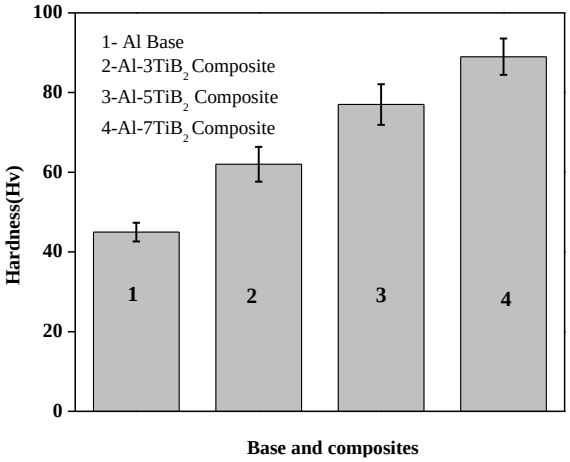


*Figure7. Vickers hardness of base and composites*

The mechanical properties of the pure Al matrix and composites are shown in Figure8. The results show that increasing $TiB_2$ content improves ultimate tensile strength and yield strength whilst decreasing ductility. The mechanical properties of the matrix were characterized with low UTS (145 $N/mm^2$) and high ductility (16.2%) due to the absence of any $TiB_2$ particles. The UTS values of 3, 5, and 7wt.%$TiB_2$composites show a 25%, 33%, and 45% improvement; and a decrease in ductility by 4.9%, 24%, and 41.3% compared to the base alloy. For the 7wt. %$TiB_2$ composite sample, a high UTS (202 $N/mm^2$) and low ductility (5.6%) were found. This increase in the UTS could be due to the load-bearing capability of the reinforcement particles. Reinforcements and dislocations caused an improvement in the resistance to crack propagation [29]. The increase in the tensile strength of the composites was mainly because of the reinforcement particles, which restricted the dislocation motion and reduced plastic deformation. A higher dislocation density resulted from the higher particle concentration. Due to the applied load, the matrix exhibited limited plastic flow. This hard reinforcement caused a backlog of dislocations. The interaction of dislocations with reinforcement and grain boundaries strengthened the alloy [30]. Shear-lag theory, described as the mechanism of load transfer from the matrix to the reinforcement particles through shear stresses at the interfaces of the composite components, could also have resulted in higher strength of the composite compared to the unreinforced matrix [31]. The reinforcing phase ($TiB_2$) is an essential load-bearing element in the matrix which facilitates the transfer of load [16].

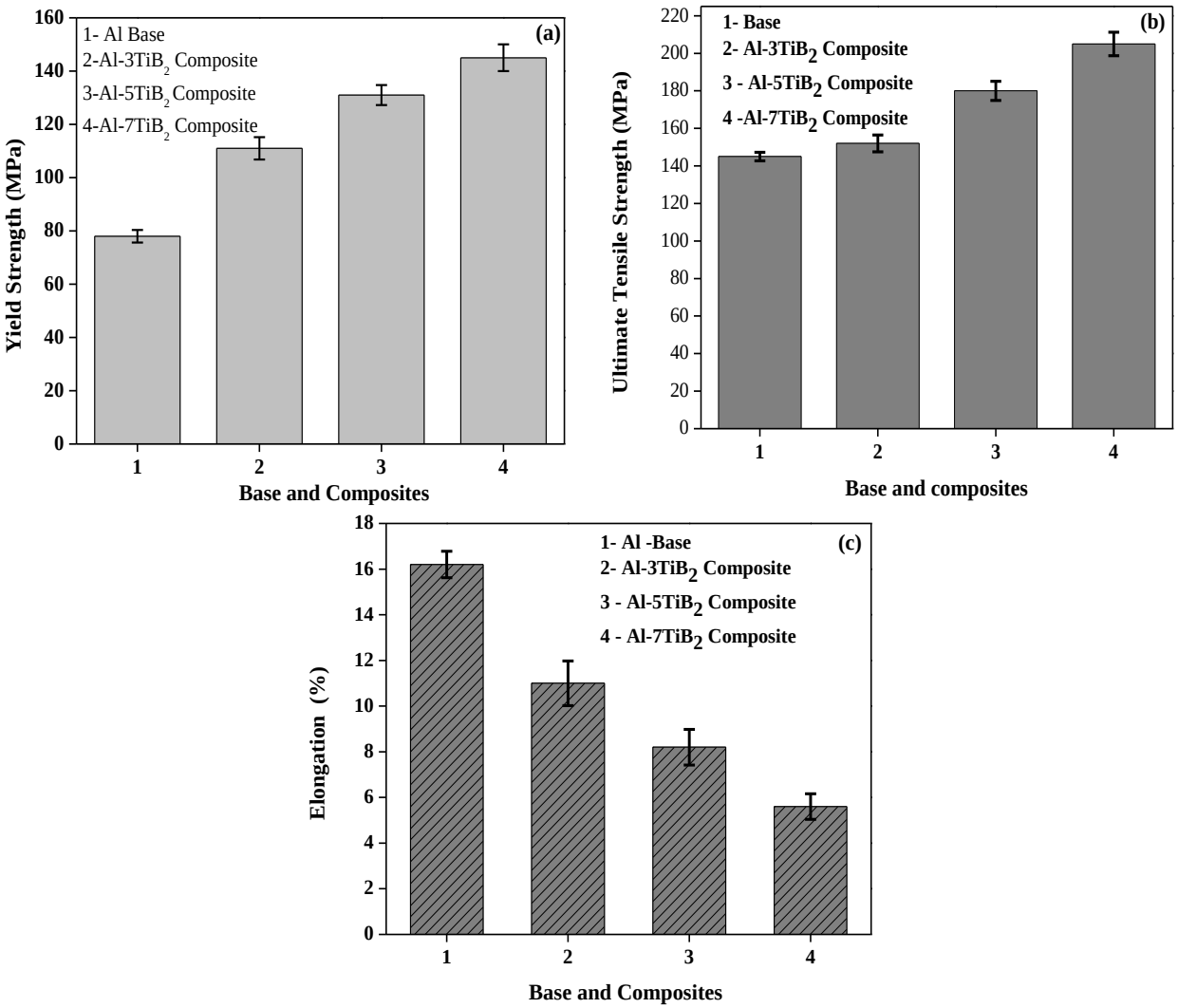


*Figure8. Tensile properties of base and composites (a)Yield strength(b)Tensile strength and (c) Elongation (%)*

### *3.3. Wear rate*

Figure 9 shows the variation of the wear rate of composites as a function of different sliding velocities and applied load conditions. The results show that at constant sliding velocities of 1, 2 and 3m/s, the wear rate shows an increasing trend with an increase in the applied load. As the load increases, considerable contact pressure and frictional heat are generated between the pin sliding face and disc, resulting in plastic deformation. A greater degree of plastic deformation may promote pin subsurface cracking, resulting in greater material removal. The increase in wear rate at higher loads can be due to $TiB_2$ particle delamination, abrasion, and chipping from the matrix. Abrasion occurs at a greater load of 40 N, where strong asperities of reinforcing particles lying between sliding faces cut and plough the pin, resulting in higher wear rates. Delamination is caused by the propagation and nucleation of cracks, and an increase in the load expedites these

mechanisms and further increases wear [32]. In the entire load varying between 10 to 40N, all three composites depict the lower wear rate at the sliding velocity of 2.0 m/s compared to 1 m/s and 3.0 m/s.

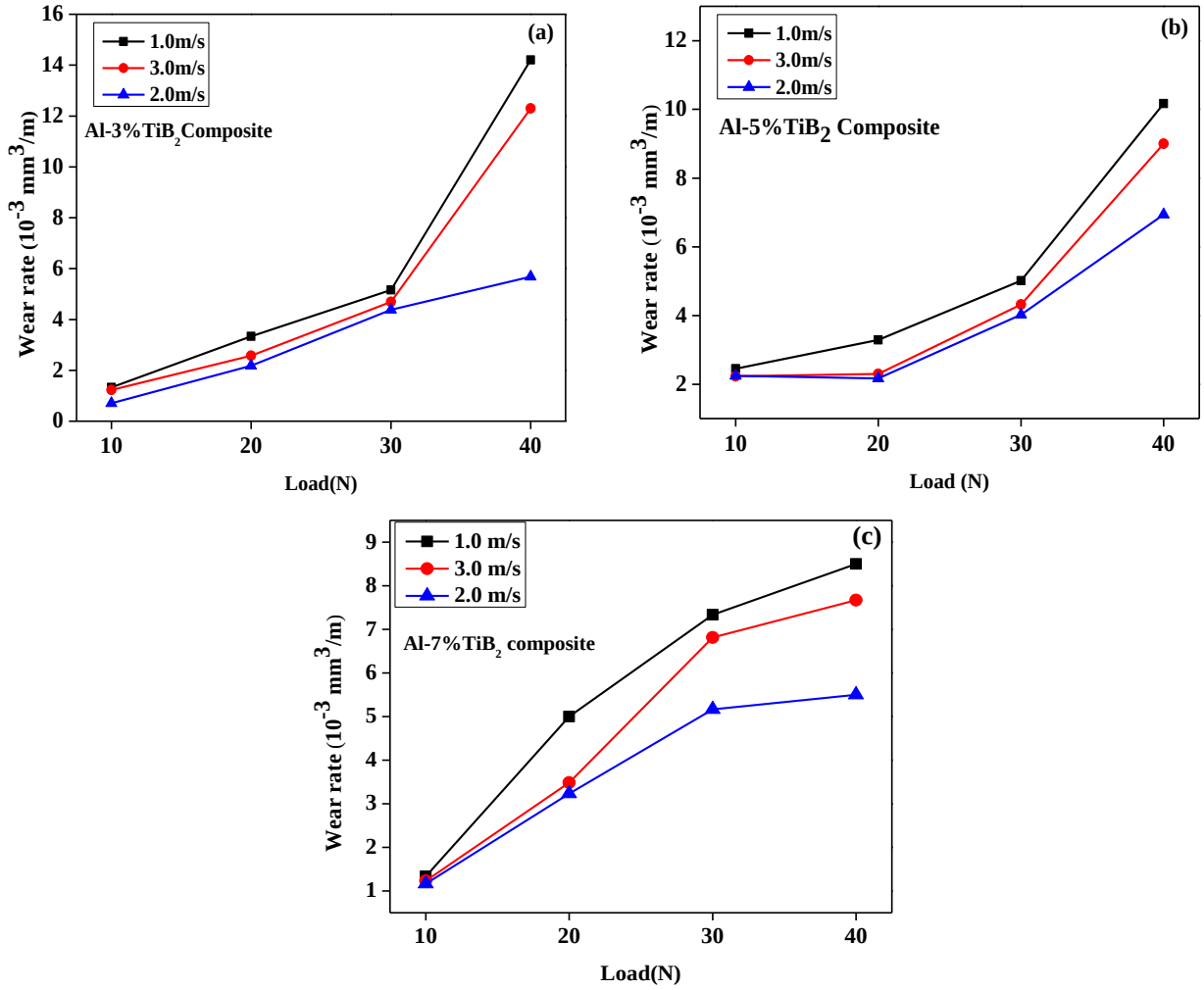


*Figure9.The variation of wear rate with the load and sliding velocity(a)Al-3wt.%$TiB_2$,(b)Al-5wt.%$TiB_2$and(c)Al-7wt.%$TiB_2$composites.*

Figure 10 displays the wear rate of the matrix and composites for different applied loads and constant sliding velocities of 1, 2 and 3m/s. It can be clearly observed that the wear decreases with the increase in $TiB_2$ content and the Al-7wt.%$TiB_2$ composite shows a lower wear rate compared to the as-cast matrix, Al-3wt.% $TiB_2$, and Al-5wt.%$TiB_2$ composites for the entire applied loads and sliding velocity conditions. Due to the high hardness and strong interfacial bonding between the in-situ reinforcement and the matrix alloy, composite materials containing a high amount of $TiB_2$ particles exhibit low wear rates.

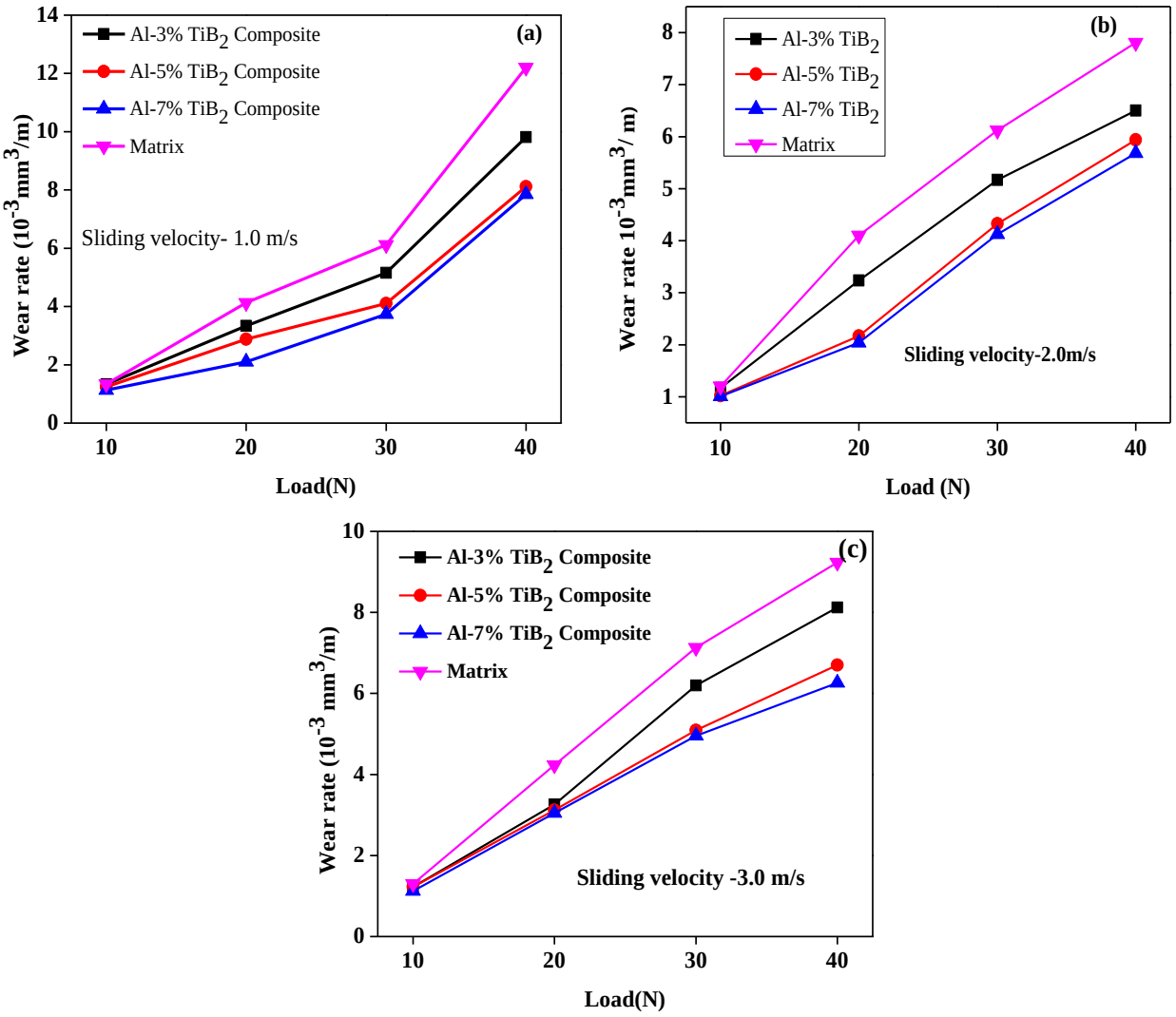


*Figure 10. The variation of the wear rate at different sliding velocity and normal load.(a)1.0(b)2.0and (c)3.0 m/s.*

Figure11depicts the variation in the wear rate with sliding speed at a fixed load of 40N for matrix and composites. The results show at a low sliding velocity of 1.0 m/s, wear rate is high and declines at a faster rate as the sliding speed is increased up to 2 m/s for both the base and composite materials. After that, the wear rate gradually increases with an increase in sliding velocity.

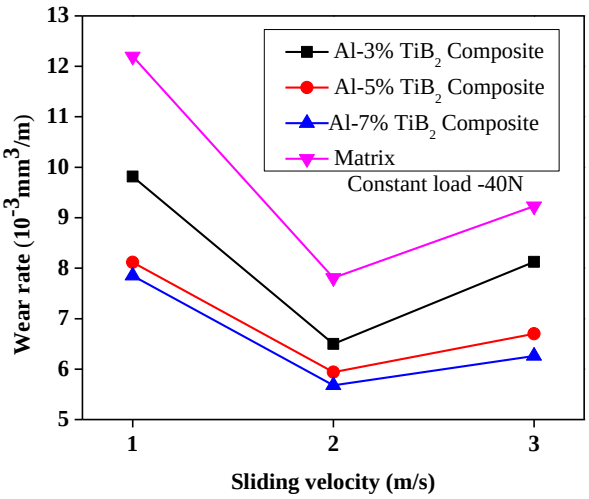


*Figure 11.The variation of the wear rate at different sliding velocity at 40N l load.*

High frictional heat is generated between the disc and the pin sliding surface as the sliding speed is increased. The material softens with increasing levels of frictional heat, which weakens the link between the matrix and the reinforcement. Material removal is made easier by the pin surface digging through tough asperities as a result of the matrix-reinforcing link being weaker. Moreover, high sliding speeds under constant loads produce high shear stresses between the pin and disc contact areas, and these high shear stresses cause hard asperities to fragment, resulting in the delamination of materials in the form of debris, which increases the wear rate [33, 34].

### *3.4. Worn surface morphology*

SEM micrographs of worn surfaces of the base and composite specimens sliding with a load of 40N and a velocity of 3.0m/s are shown in Figure 12. The matrix of worn-out surface (Figure 12a) shows adhesive marks and large plastic deformation, wear sheets or laminates as well as numerous pits, and cracks. Delamination wear was indeed caused by the formation and propagation of a subsurface crack perpendicular to the sliding direction, resulting in loose wear sheets or laminates. Plastic deformation leads to material ploughing and severe delamination. Higher amounts of particles from the delamination are dislodged along their sides by the sliding asperities. The increased friction force causes more frictional heat to be generated at higher speeds and loads, resulting in plastic deformation of the base material. High ductility material is more prone to adhesive wear due to the development of cracks that connect and cause a detachment of the material [35]. Al-3wt. %$TiB_2$ composite worn surface is shown in Figure 12b. A combination of abrasive and delamination wear is evident with small, exposed cracks, deep

abrasive grooves, and material dislodging along the sliding direction. On the other hand, the worn surface of the Al-5wt.%$TiB_2$composite (Figure 12c) consists of long parallel grooves along the sliding direction, which are caused by the abrasion of entrapped particles, are clearly visible. From the SEM micrographs, it can be concluded that with an increase in wt.% $TiB_2$ particles, abrasive grooves become increasingly shallow, and smoothening is seen, indicating an improvement in the wear resistance. The worn surface Al-7wt.%$TiB_2$ composite (Figure 12d) appears smooth and consists a white layer representing oxidative wear. During sliding, frictional heat generated between the mated surfaces leads to oxidation. Figure 12d also depicts worn surfaces with visible micro-pits and smooth grooves in the direction of sliding. In addition, the wear scars on the Al-7wt.%$TiB_2$ composite surface were smoother than those on the surfaces made of base material, Al-3wt.$TiB_2$, and Al-5wt.$TiB_2$.

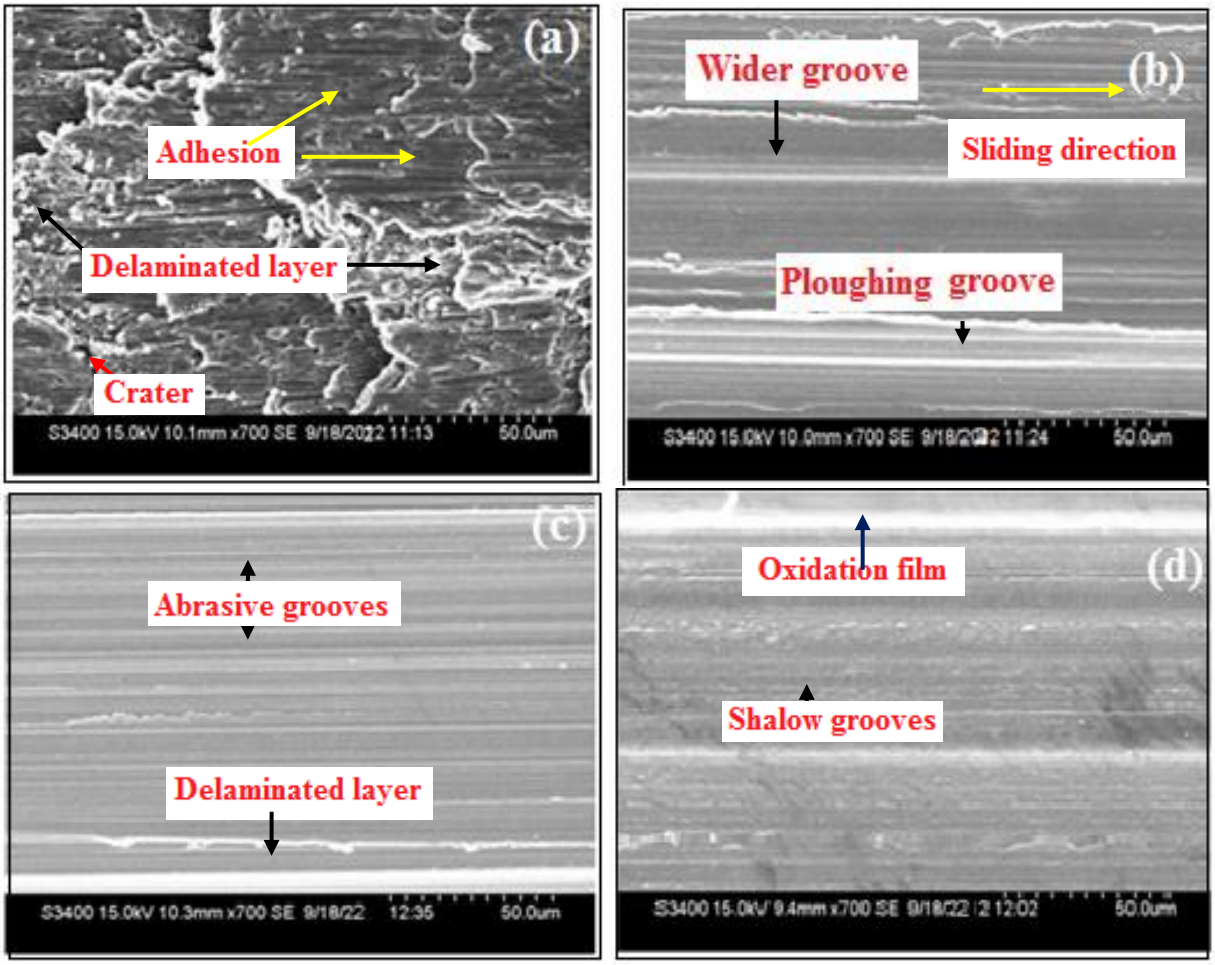


*Figure12.SEM plan micrographs of the worn surfaces of (a) Matrix (b) Al- 3%$TiB_2$,(c) Al-5%$TiB_2$and(d)Al-7%$TiB_2$ composites at load of 40N load and 3.0m/s siding velocity.*

The direct metal-to-metal contact between the pin surfaces and a steel disc is greatly reduced by the creation of an oxide layer, which lowers the wear rate. The Al-7% $TiB_2$ composite have more resilience to the indentation due to the high content of $TiB_2$ particles that serve as the worn surface appears smooth and has a thicker oxidative layer. Composites offer superior resistance to thermally induced deformation compared to the base owing to the presence of $TiB_2$ particles prevent thermal softening of the matrix resulting in better wear resistance in the composite materials. In summary, it can be concluded that the Al-7wt.%$TiB_2$ composite exhibits exceptional wear resistance qualities suitable for tribological applications.

## 4. Conclusion

Al*x*$TiB_2$ (*x*=3, 5, and 7wt. %) composites were produced in this study by reacting $KBF_4$and $K_2TiF_6$with melted aluminum. The effects of $TiB_2$contenton the microstructures, hardness, and sliding wear behavior of the resulting composites are investigated. The following conclusions can be drawn from the findings of this research.

(1) The microstructure of the in-situ composites shows that very fine $TiB_2$ particles are formed in the range of 0.5-10 μm and nearly uniformly distributed at the grain boundaries and within the Al grains of the α-Al matrix. It has also been found clustering of $TiB_2$ particles with a higher $TiB_2$ content.

(2) The addition of $TiB_2$ particles in the Al matrix improved hardness and tensile strength of the Al matrix while decreasing its ductility.

(3) The wear resistance of the composites is higher than that of the basic alloy, and the wear rate decreases as the $TiB_2$ percentage in the composites increases.

(4) The wear rate gradually increased with the increasing loads. On the other hand, the wear rate decreased as the sliding velocity increased from 1.0 m/sec to 2.0 m/sec but increased as the sliding velocity was further increased to 3 m/sec.

(5) The matrix and composites have been impacted by the three main categories of wear mechanisms: adhesive, oxidative, and abrasive. Adhesive wear is the primary wear mechanism of the matrix. This is reflected in the matrix worn surface by the presence of scoring and the transfer of material from the disc to the load bearing surface. Oxidative wear is more prevalent in composites, as evidenced by a worn surface of the composite with an oxide layer, a smooth surface, and small abrasive grooves filled with oxides.

**Acknowledgements**

The authors would like to thank the Mechanical Department of Tontadarya College of Engineering, Gadag for providing necessary facilities and support for this work.

**References**

[1]. Lakshmikanthan A, Angadi S, MalikV,Saxena KK,Prakash C, Dixit S, Mohammed,KA. Mechanical and Tribological Properties of Aluminum-Based Metal-Matrix Composites. Materials.2022, 15, 6111. https://doi.org/10.3390/ma151761112.

[2]Bala Narasimha Guniputi, Pratheep Reddy T and Vamsi Krishna Mamidi. Effect of in-situ reaction time on the strength of AA5052/ZrAl3 metal matrix nano composites. Advances in Materials and Processing Technologies.2022. 10.1080/2374068X.2022.2091188.

[3]Ronald G. Munro. Material Properties of Titanium Diboride. [J. Res. Natl. Inst. Stand. Technol.2000;105:709-720.

[4]Karbalaei AkbariM,H.R. Baharvandi HR,. Shirvanimoghaddam K. Tensile and fracture behavior of nano/micro TiB2 particle reinforcedcasting A356 aluminum alloy composites. 2015,Materials and Design; 66:150–161.

[5]Hashim J, Looney L, Hashmi MSJ. The wettability of SiC particles by molten aluminum alloy. J Mater Process Technol 2001; 119:324–328.

[6] Gebre Fenta Aynalem. Processing Methods and Mechanical Properties of Aluminium Matrix Composites. Advances in Materials Science and Engineering.2020. https://doi.org/10.1155/2020/3765791

[7]Yutao Zhao.In-Situ Synthesis of Aluminum Matrix Composites. In-Situ Synthesis of Aluminum Matrix Composites, 2022. Publisher: Springer

[8] LakshmiS ,Lu L, GuptaM.In situ preparation of $TiB_2$ reinforced Al based composites. Journal of Materials Processing Technology.1998;73,1–3:160-166. https://doi.org/10.1016/S0924-0136(97) 00225-2

[9] Kori SA , Auradi V. Influence of reaction temperature for the manufacturing of Al-3Ti and Al-3B master alloys and their grain refining efficiency on a Al-7Si alloy, Advanced Materials Research, 2007;29:111-115

[10]Niranjan K, Lakshminarayanan P R, Dry Sliding Wear Behavior of In Situ Al-$TiB_2$Composites, Mater. Des., 2013;47:167–173

[11] Feng C.F, Froyen L. Microstructures of in situ Al/TiB2 MMCs prepared by a casting route. Journal of Materials Science .2000;35:837–850. https://doi.org/10.1023/A:1004729920354

[12] Kumar S, Chakraborty M, Subramanian Sarma V,Murty BS.Tensile and wear behaviour of in situ Al–7Si/$TiB_2$ particulate composites. Wear. 2008; 265,1–2,25:134-142.

[13]Ze-You Chen,Yuyong Chen, An GY, Shu Q. Microstructure and properties of In situ Al/$TiB_2$ composite fabricated by in-melt reaction method. Metallurgical, 2000; 31(8):1959-1964

[14] Manoj M, Suresh Kumar J, Mugendiran V.Effect of TiB2 particles on the morphological, mechanical and corrosion behaviour of Al-7075 metal matrix composite produced using stir

casting process. International Journal of Metal casting. 2021, https://doi.org/10.1007/s40962-021-00696-3.

[15] Pramod SL, Srinivasa R. Bakshi,Murty B S. Aluminum-Based Cast In Situ Composites: A Review. Journal of Materials Engineering and Performance.2015. 10.1007/s11665-015-1424-2

[16] Kedarnath Rane, Narendra Dhokey.On the Formation and Distribution of In Situ Synthesized $TiB_2$ Reinforcements in Cast Aluminium Matrix Composites. J. composite science.2018; 2, 52:1-11. Doi:10.3390/jcs2030052.

[17] Madhavan S, Balasivanandha Prabu S, Padmanabhan K.A. On the role of process parameters of aluminothermic reaction synthesis of in-situ Al-TiB2 composites: microstructure and mechanical properties.Letters on Materials.2014; 4,2:84-88

[18] Zhengcai Liu, Tao Zhu, Yiwang Jia, Dongfu Song, Nan Zhou,Kaihong Zheng.Preparation of in-situ TiB2 reinforced aluminum matrix composites assisted by two steps of ultrasonic vibration Mater. Res. Express 8 (2021)046506. DOI 10.1088/2053-1591/abea5a.

[19] Mallikarjuna C,Shashidhara SM, Mallik US, Parashivamurthy KI.Grain refinement and wear properties evaluation of aluminum alloy 2014 matrix-$TiB_2$ in-situ composites, Materials & Design.2011;32,6:3554-3559.

[20] Weiguo Wu, Tiancheng Zeng, Wenfeng Hao, Shiping Jiang.Microstructure and Mechanical Properties of Aluminum Matrix Composites Reinforced With In-Situ TiB2Particles. Front. Mater.2022,2 https://doi.org/10.3389/fmats.2022.817376.

[21] Sudhir Kumar, Rupinder Singh, Hashmi M. S. J (2020) Metal matrixcomposite: a methodological review, Advances in Materials and Processing Technologies, 6:1:13-24. DOI: 10.1080/2374068X.2019.1682296

[22] Arvind Sankhla and Kaushik M Patel Metal Matrix Composites Fabricated by Stir Casting Process–A Review. Advances in Materials and Processing Technologies

2022; 8,2: 1270–1291.https://doi.org/10.1080/2374068X.2020.1855404.

[23] Malkiya R. et al. Mechanical and wear behavior of TiB2-B4C reinforced Al7075 alloy hybrid composites for aerospace applications, Advances in Materials and Processing Technologies,2022; 8:4, 4209-4228, DOI:10.1080/2374068X.2022.2050043.

[24] Tee Kl, Lu L,Lai MO. In situ stir cast Al-TiB2 Composite: processing and mechanical properties. Materials Science and Technology.2013;17:2:201-206, DOI:10.1179/026708301101509863.

[25] Vinayagam Mohanave et al. Investigation on Inorganic Salts K2TiF6 and KBF4 to Develop Nanoparticles Based $TiB_2$ Reinforcement Aluminium Composites.J. Bioinorganic Chemistry and Applications e 2022,13 pages https://doi.org/10.1155/2022/8559402

[26] Fei Chen et al. $TiB_2$ reinforced aluminum based in situ composites fabricated by stir casting,Materials Science & Engineering A,2015 .625:357-368. https://doi.org/10.1016/j.msea.2014.12.033.

[27] Bartels, C., Raabe, D., Gottstein, G., and Huber, U.Investigation of the Precipitation Kinetics in an A16061/TiB2 Metal Matrix Composite. Mater. Sci. Eng. A. 1997;237,1, :12–23. doi:10.1016/s0921-5093(97)00104-4

[28] Pengchao Zhang, Jinchuan Jie, Hang Li,Tongmin Wang, Tingju Li. Microstructure and properties of $TiB_2$ particles reinforced Cu–Cr matrix composite, J Mater Sci. 2015.50:3320–3328 DOI 10.1007/s10853-014-8762-6.

[29] Naresh Mallireddy, Siva K.Investigation of Microstructural, Mechanical and Corrosion Properties of AA7010-$TiB_2$ in-situ Metal Matrix Composite.Sci Eng Compos Mater 2020; 27:97–107. https://doi.org/10.1515/secm-2020-0010.

[30] Aikin R M, Jr. The Mechanical Properties of In-Situ Composites. The JOM,1997;49,8:35-39.

[31] Mohammad Narimani, Behnam Lotfi, Zohreh Sadeghian,Investigating the microstructure and mechanical properties of Al-$TiB_2$ composite fabricated by Friction Stir Processing. Materials Science & Engineering A. doi.org/10.1016/j.msea.2016.07.086

[32] Dipankar Dey, Abhijit Bhowmik, Ajay Biswas. Influence of $TiB_2$ addition on friction and wear behaviour of Al2024−TiB2 ex-situ composites.Trans. Nonferrous Met. Soc. China.2021;31:1249−1261.

[33] Ramesh C S, Ahamed A. Friction and wear behaviour of cast Al6063 based in situ metal matrix composites J. Wear, 2011, 271: 1928-1939.

[34]Hullur MK, Dayanand M Goudar, Venkateshwaralu K, Kori SA.Sliding Wear Behaviour of In Situ $TiB_2$Reinforced Hypoeutectic Al-Si Alloy Composites.International Journal ofMetalcasting.2022; DOI: https://doi.org/10.1007/s40962-022-00847-0

[35] Singh R, Shadab M, Dash A, Rai R N. Characterization of dry sliding wear mechanisms of AA5083/B4C metal matrix composite [J]. Journal of the Brazilian Society of Mechanical Sciences and Engineering, 2019, 41: 98−109.